

1 **Polar organic chemical integrative sampler (POCIS) allows compound**
2 **specific isotope analysis of substituted chlorobenzenes at trace levels**

3
4 Shamsunnahar Suchana^a, Sávia Gavazza^b, Natanna Melo^b, Elizabeth Edwards^c,
5 Line Lomheim^c, E. Erin Mack^d, and Elodie Passeport^{a,c*}

6
7 ^aDepartment of Civil & Mineral Engineering, University of Toronto

8 35 St. George Street, Toronto, Ontario, M5S 1A4, Canada

9 ^bLaboratório de Saneamento Ambiental, Departamento de Engenharia Civil e Ambiental,

10 Universidade Federal de Pernambuco, Recife, PE, 50740-530, Brazil

11 ^cDepartment of Chemical Engineering & Applied Chemistry, University of Toronto

12 200 College Street, Toronto, Ontario, M5S 3E5, Canada

13 ^dDuPont, Wilmington, DE 19805, United States

14
15 *Corresponding author: elodie.passeport@utoronto.ca, +1 416-978-5747

16
17
18 **Abstract**

19 Compound specific isotope analysis (CSIA) is an established tool to demonstrate *in situ*
20 degradation of traditional groundwater contaminants at heavily contaminated sites, usually at
21 mg/L range aqueous concentrations. Currently, an efficient preconcentration method is lacking to
22 expand CSIA to low aqueous concentration environmental samples. This work demonstrated the
23 compatibility of polar organic chemical integrative sampler (POCIS) with CSIA of C, H, and N
24 isotopes for four NH₂- and NO₂-substituted chlorobenzenes at low µg/L. Diffusion and sorption
25 showed insignificant carbon isotope fractionation (<0.7‰) in laboratory experiment, except for a
26 reproducible shift of 1.6‰ for 3,4-dichloronitrobenzene. A similar constant reproducible shift of
27 0.8-2‰ was evident for N-CSIA. Whereas, the compatibility of POCIS for H-CSIA seems to be
28 analyte specific possibly reflecting the adsorption mechanism to POCIS by H-bonding.
29 Performance of the POCIS-CSIA method was evaluated in a pilot constructed wetland where
30 comparable C- and N-CSIA results were obtained from grab sampling and POCIS. This work
31 opens the potential of CSIA application to the low concentration polar emerging contaminants in
32 the environment, such as pesticides, pharmaceuticals, and flame-retardants.

33

34 **Keywords: POCIS; CSIA; isotope analysis; chloronitrobenzenes; passive sampling**

35

36 **1. Introduction**

37 Substituted chloronitrobenzenes, chloroanilines, and nitrotoluenes are common source materials
38 to produce various pesticides, dyes, explosives, pharmaceuticals, personal care products,
39 preservatives, and antioxidants.¹ Chloroanilines can be formed in the natural environment by
40 biotic and abiotic processes during the reductive transformation of chloronitrobenzenes,^{2,3} and

41 transformation of several phenylurea herbicides, such as diuron, linuron, neburon, and monuron.⁴
42 Microbial oxidation of chloroanilines by soil fungus can also form chloronitrobenzenes.⁵
43 Nitrotoluenes are primary by-products of explosives and found extensively at former munition
44 sites.¹ Many of these compounds are acutely toxic, mutagenic, carcinogenic, and listed on the
45 United States Environmental Protection Agency's list of priority pollutants.⁶ Due to their
46 persistence in the environment,⁷ they are detected in industrial wastewaters and natural water
47 bodies in various regions.^{8,9}

48 Conventionally, contaminant fate in the environment is evaluated by monitoring the changes in
49 their *in situ* concentrations. However, concentration-based approaches cannot provide
50 unequivocal evidence of *in situ* degradation as non-destructive processes, e.g., sorption,
51 volatilization, and dilution, can also affect concentration. Compound specific isotope analysis
52 (CSIA) has the potential to distinguish between destructive and non-destructive processes *in situ*
53 by measuring the changes in the ratio of a heavy (e.g., ¹³C) and a light (e.g., ¹²C) stable isotopes
54 of an element (e.g., C) in a molecule.¹⁰ Physical processes do not involve bond cleavage,
55 typically resulting in negligible isotope fractionation.^{11–13} CSIA has been used as a direct line of
56 evidence for *in situ* degradation of many organic compounds.¹⁰ However, due to the high
57 instrumental detection limits of isotope ratio mass spectrometers (IRMS), CSIA has been mainly
58 limited to contaminated sites with high µg/L to mg/L range concentrations.¹⁰ Recent applications
59 of CSIA to µg/L to higher ng/L concentrations have been made after extracting 10 to 100 L of
60 water for each analysis using solid-phase extraction (SPE).^{14,15} Using large volume SPE is
61 susceptible to preconcentrate co-contaminations and background matrix. Besides, significant
62 isotope fractionation (up to 6‰) was observed for the extraction of more than 10 L.¹⁴ Thus, an
63 efficient preconcentration technique for trace contaminants in water free from method-induced

64 isotope fractionation is necessary to expand CSIA for low concentration environmental samples,
65 such as long-term monitoring groundwater sites and surface water environments where
66 concentrations are often more diluted.

67 Combining passive integrative sampling with CSIA could be an effective *in situ* preconcentration
68 technique that requires little effort during sample preparation. Although various *in situ* passive
69 sampling techniques are widely accepted, limited research, to date, has explored their
70 compatibility with CSIA. Wang et al. (2004) reported negligible C and H isotope fractionation of
71 several polycyclic aromatic hydrocarbons using semi-permeable membrane devices under
72 different exposure conditions.¹⁶ Another permeation-based passive sampler known as the
73 Waterloo Membrane Sampler was evaluated for sorption- and desorption-associated C isotope
74 fractionation for gas-phase hydrocarbon sampling¹⁷ and was successfully applied at
75 contaminated sites.^{17,18} A type of diffusion passive sampler, called peeper, also showed no
76 significant C isotope fractionation for aromatic and chlorinated aromatic compounds,¹⁹ and was
77 successfully deployed in sediments to track pore water benzene and chlorobenzene natural
78 attenuation by CSIA.^{20,21} Until today, no passive sampling technique has been validated for
79 CSIA targeting trace polar organic compounds, such as pesticides, pharmaceuticals, and personal
80 care products. The polar organic chemical integrative sampler (POCIS), introduced by Alvarez et
81 al. in 2004, consists of a sorbent phase sandwiched between two polyethersulfone membrane
82 filters.²² POCIS involves multiphase analyte mass transfer from the water column to the sampler
83 receiving phases via diffusion and adsorption, which can potentially cause isotope fractionation.
84 Thus, a careful evaluation of the sampling method is critical to ensure that the original isotope
85 signature of the analytes are conserved in POCIS.

86 The main objective of this work was to evaluate the compatibility of POCIS with CSIA to
87 monitor *in situ* transformation of the target compound groups at a contaminated industrial site.
88 Because POCIS has never been applied for most of the target compounds, we first evaluated
89 whether POCIS can accumulate enough analyte mass for CSIA application. Second, we
90 evaluated method-induced isotope fractionation during sampling and post-processing phases
91 using laboratory experiments. Third, we demonstrated the performance of the POCIS-CSIA
92 method in at a field pilot constructed wetland system.

93

94 **2. Materials and methods**

95 **2.1 Chemicals and materials**

96 All chemical details are given in Supporting Information (SI) Section S1. Selected analytes have
97 been abbreviated as follows: 2-nitrotoluene (2-NT), 2- and 4-chloronitrobenzene (2-CNB and 4-
98 CNB), 4-chloroaniline (4-CA), 2,3- and 3,4-dichloroaniline (2,3-DCA and 3,4-DCA), and 2,5-
99 and 3,4-dichloronitrobenzene (2,5-DCNB and 3,4-DCNB). 2,5-DCNB was used as an internal
100 standard to correct for potential losses during sample processing.

101 All POCIS were assembled using OASIS HLB bulk sorbent (30 μm particle size, divinylbenzene
102 N-vinyl-pyrrolidone, Waters, Massachusetts, USA) and polyethersulfone (PES) microporous
103 membrane disk filters (0.1 μm pore size, 90 mm diameter, PAL Corporation, California, USA)
104 following standard configuration.²³ Details on POCIS preparation and pre-treatment are given in
105 Suchana et al (modeling paper) and briefly described in Section S2.

106 **2.2 POCIS laboratory experimental systems**

107 Three experiments were performed statically without renewal of the analytes in large glass jars
108 (diameter: 19 cm, height: 26 cm, total capacity: 7.5 L) as detailed in Suchana et al. (modeling
109 paper). Static experimental setup was chosen over continuous flow-through systems to avoid
110 isotope dilution.

111 First, a preliminary exposure experiment was conducted to verify the potential of POCIS to
112 accumulate the target compounds for CSIA. For that, 7 L of autoclaved ultrapure water
113 (resistivity of 18.2 MΩcm) was spiked at a target initial concentration of 1 mg/L for each 4-
114 CNB, 3,4-DCNB, 4-CA, and 3,4-DCA using methanol stock (<0.5% v/v of methanol). The
115 system was mixed and left untouched for 24 h to allow for analyte dispersion. Then, one POCIS
116 was suspended vertically in each jar from the top (membrane exposure level 4.5-5.0 cm from
117 bottom) using a stainless-steel wire loop. The deployment of the POCIS defined the start of the
118 experiment, i.e., time 0. On day 44 since the start of the experiment, water sample was collected
119 for concentration analysis, and POCIS HLB and PES phases were extracted separately to
120 quantify the accumulated analytes.

121 Second, a kinetic experiment was performed using a sacrificial setup with one POCIS per jar,
122 each filled with 6 L of autoclaved ultrapure water. Each jar was spiked with an initial target
123 concentration of 10 mg/L for each analyte as before. Note that 2-NT was spiked instead of 4-CA
124 in the second experiment to obtain a complete separation in the isotopic trace in the IRMS. A
125 relatively high initial concentration was used to ensure sufficient mass accumulation in POCIS
126 for CSIA at six sampling times. After 24 h of spiking, water from the top and bottom of each jar
127 was analyzed immediately to confirm the system was well mixed and determine the initial
128 spiking concentration in each setup. One POCIS was deployed in each setup (i.e., time 0), and
129 duplicate POCIS were sacrificed at days 7, 14, 21, 31, 45, and 60. At each time point, water

130 samples were also collected for concentration and isotope analyses. Analyte mass balance in
131 sacrificial setup was calculated at each time point (Section S3).

132 Third, another kinetic experiment was conducted identical to the second experiment, except that
133 no HLB sorbent was placed inside the two PES membranes of a POCIS configuration. This
134 experiment was performed to quantify analyte isotope fractionation induced by diffusion through
135 and adsorption on the PES membrane. On day 60, the PES membranes were extracted for both
136 concentration and isotope analyses.

137

138 **2.3 POCIS deployment in the field**

139 POCIS were deployed at a pilot surface flow constructed wetland system for 60 days. The
140 wetland system was continuously fed by partially-treated groundwater from an industrial site
141 contaminated with the target compounds. Six POCIS were deployed including three POCIS
142 protected with conventional stainless-steel mesh and three POCIS protected with a copper mesh
143 to act as an antimicrobial metal.²⁴ In addition, two separate POCIS, one in each casing material,
144 were deployed to evaluate the potential of biofilm growth on the outer membrane surface during
145 the exposure period (referred to as “biofilm POCIS”). Isotope signatures from POCIS were
146 compared with that of the 4 L grab sample preconcentrated by SPE using the method described
147 in Suchana et al. SPE/CSIA paper. After retrieval, all POCIS were wrapped separately and stored
148 at -20°C until further processing.

149

150 **2.4 Controls and blanks**

151 For laboratory experiments, duplicate negative controls were prepared by deploying one POCIS
152 in an analyte-free jar to assess contamination during deployment and sample processing.
153 Duplicate positive controls were prepared with ultrapure spiked water and POCIS metal parts
154 only (i.e., no membrane and no sorbent) to monitor contaminant loss due to processes other than
155 POCIS uptake, such as volatilization and sorption to the experimental setup. Duplicate POCIS
156 fabrication blanks (i.e., not deployed in water but that underwent the same preparation steps)
157 were also used to evaluate potential contamination during POCIS preparation. For field POCIS,
158 an additional trip blank (i.e., taken to the field during the deployment and retrieval but never
159 opened), and separate deployment and retrieval blanks (i.e., taken to the field and exposed to the
160 air during the deployment and retrieval, respectively) were used to evaluate potential
161 contamination during sampling.

162

163 **2.5 Sample processing for concentration and isotope analyses**

164 Water samples from Experiment 1 were analyzed after filtration through 0.22 μm syringe filter
165 (PTFE, Chromspec, ON, Canada) without further processing. For Experiment 2, water was
166 extracted at each time point by OASIS HLB SPE cartridge (6 mL, 30 μm particle size, 200 mg
167 sorbent, Waters) for both concentration and isotope analyses following the method described in
168 Suchana et al. SPE-CSIA paper. Extraction of PES phase was performed following Suchana et
169 al. modeling paper.

170 For concentration analysis using SPE, HLB, and PES extracts (ethyl acetate), a suitable aliquot
171 (dilution factor 100 to 1000) was mixed with ultrapure water to obtain concentrations within the
172 instrumental calibration range. Due to the limited water solubility of ethyl acetate (<8% v/v),

173 samples were prepared by adding <5% (v/v ethyl acetate:water) of the final extract to ultrapure
174 water. For isotope analysis, ethyl acetate extracts were injected directly or diluted, if necessary,
175 for a splitless injection.

176 For field POCIS, the outer membrane surface was first washed thoroughly using ultrapure MQ
177 water and then both the HLB and PES phases were processed as before for isotope analysis.

178 Extraction of field water collected using grab sampling was performed by SPE (Suchana et al.
179 SPE/CSIA paper). All extracts were stored at -20°C until analysis. All extraction methods are
180 briefly described in Section S4.

181

182 **2.6 DNA extraction and scanning electron microscopy of field POCIS**

183 The two PES membranes of the biofilm POCIS were collected at day 60 of the field exposure,
184 rinsed with ultrapure water to remove large unattached particles, and then processed for both
185 DNA extraction (one membrane) and scanning electron microscopy (the other membrane).

186 The central exposed circle of the membrane and the donut shaped outer part that was under the
187 metal ring were cut into small pieces using a sterile slide, and transferred to a microcentrifuge
188 tube for DNA extraction following the PowerSoil™ Kit protocol (Mo Bio Laboratories Inc.
189 Carlsbad, CA, USA). DNA extracts were sequenced for the 16SrRNA gene using the MiSeq
190 Sequencing System equipment (Illumina Inc., USA). Details are given in Section S5.

191 The morphologies attached to the PES membranes of POCIS were observed by scanning electron
192 microscopy (JEOL®6390LV, JEOL Ltda., Tokyo, Japan), with 10 kV of acceleration voltage.
193 Similarly as DNA extraction, both the exposed and outer part of the membrane were collected

194 separately, dried at room temperature, and coated with a fine gold layer for 5 minutes, using the
195 Denton Vacuum IV metallizer device, before visualization.

196

197 **2.7 Analytical methods**

198 *Concentration analysis*

199 A Dionex Ultimate 3000 series High-Performance Liquid Chromatography (HPLC) connected
200 with a diode array detector (DAD) was used for concentration determination of laboratory
201 samples (Suchana et al. modeling paper). Concentration analysis of the field samples was
202 performed using xxx. Details are given in Section S6.

203 *Compound specific carbon isotope analysis*

204 Isotope signatures ($\delta^{13}\text{C}$, $\delta^{15}\text{N}$, and $\delta^2\text{H}$) were measured using a TRACE 1300 gas
205 chromatograph (GC) coupled with an isotope ratio mass spectrometer (IRMS, Delta V plus,
206 Thermo Scientific). Conversion of analytes to the measurement gas for C- and N-CSIA (e.g.,
207 CO_2 and N_2) was performed in a commercial NiO/CuO/NiO-tube reactor (Isomass Scientific
208 Inc., Alberta, Canada) operated at 1000°C. Measurement of H isotope was performed using
209 custom-made chromium-based high-temperature conversion reactor (Cr/HTC) operated at
210 1200°C. Details on chromatographic parameters are given in Suchana et al. (SPE paper).

211 The isotope signature of the pure compounds was determined in an elemental analyzer (EA)
212 coupled with an IRMS at the Helmholtz Centre for Environmental Research (UFZ) in Leipzig,
213 Germany. Isotope measurement of the experimental samples was bracketed with that of the
214 characterized pure standards. All reported values were normalized using a multi-point calibration

215 of in-house reference standards. The measured $\delta^{13}\text{C}$ values were considered accurate if the
216 bracketed standards were within $\pm 0.5\text{‰}$ from their characterized values, considering a total
217 analytical uncertainty of $\pm 0.5\text{‰}$.²⁵ A total analytical uncertainty of $\pm 0.5\text{‰}$ and $\pm 10\text{‰}$ was
218 accepted for N and H isotopes, respectively (Suchana et al. SPE paper).

219 The change in isotope signature of the experimental samples was expressed as the differences of
220 the measured δ values by GC/IRMS from that of the reference standards measured in EA/IRMS,
221 i.e., $\Delta\delta_{\text{Sample}} = \delta_{\text{EA/IRMS}} - \delta_{\text{GC/IRMS}}$. All values were reported in per mill (‰), equivalent to
222 MilliUrey (mUr)²⁶, and relative to the international standards of Vienna PeeDee Belemnite,
223 Vienna standard mean ocean water, and air for carbon, hydrogen, and nitrogen, respectively.

224

225 **2.8 Method quantification limit**

226 The method quantification limit of the POCIS-CSIA method depends on the sampler-water
227 partition of analytes (equilibrium sampling regime) or the sampling rate (kinetic sampling
228 regime) in POCIS and the instrumental detection limits of the IRMS. Details are provided in
229 Section S7.

230

231 **3. Results**

232 **3.1 Analyte accumulation in POCIS for CSIA**

233 Overall, a significant accumulation of all target analytes was observed in both HLB and PES
234 phases from Experiment 1 (Figure S1, Section S8). Between 1580 (3,4-DCNB) to 4860 nmol (4-
235 CA) accumulated in the HLB sorbent; whereas, the PES membranes accumulated on average

2430 nmol of 4-CA, 4-CNB, and 3,4-DCNB and 5180 nmol of 3,4-DCA. Accumulation in the HLB sorbent was 1.7 to 1.9 times higher than that of the PES membranes for monochlorinated compounds, i.e., 4-CA and 4-CNB. Dichlorinated compounds, i.e., 3,4-DCA and 3,4-DCNB, accumulated preferentially in the PES membranes. For a final 1.5 mL extract volume and standard splitless 1- μ L solvent injection in the GC, between 6 (3,4-DCNB, HLB sorbent phase alone) and 20 nmol of C (3,4-DCA, PES membrane phase alone) can be injected on column. If the two phases are pooled and the extracts prepared and injected under the same conditions, even higher amounts of C can be obtained from one POCIS, i.e. from 16 (3,4-DCNB) to 36 nmol (3,4-DCA) of C. In the field, larger analyte accumulation can be expected due to advection processes.²²

246

247 **3.2 POCIS kinetic experiments**

248 Figure 1 shows the analyte mass and corresponding $\delta^{13}\text{C}$, $\delta^{15}\text{N}$, and $\delta^2\text{H}$ profiles over the course
249 of the experiments in the water and POCIS sorbent and membrane phases (Experiment 2).

250 *Analyte mass profile*

251 A decrease of analytes from the water phase and accumulation in POCIS was observed over time
252 from each sacrificial setup (Figure 1a-1d). After 60 days, the initial spiked mass of 2-NT, 4-
253 CNB, and 3,4-DCA decreased by 21-22% and that of 3,4-DCNB decreased by 44% in the water
254 phase. We considered that adsorption equilibrium was reached when less than 2% of the analyte
255 mass in the water phase changed between two consecutive sampling times. While concentration
256 equilibrium was apparent at day 45 for 2-NT, 4-CNB, and 3,4-DCA, the mass of 3,4-DCNB in
257 water decreased by 6% between day 45 and 60, indicating non-equilibrium adsorption on

258 POCIS. However, this 6% decrease in 3,4-DCNB mass was mainly due to the HLB phase (93%
259 of the total mass decrease) while additional adsorption on PES was negligible (Figure 1d). Thus,
260 over a 2-month deployment period, adsorption of 3,4-DCNB might reach an equilibrium only on
261 the PES phase.

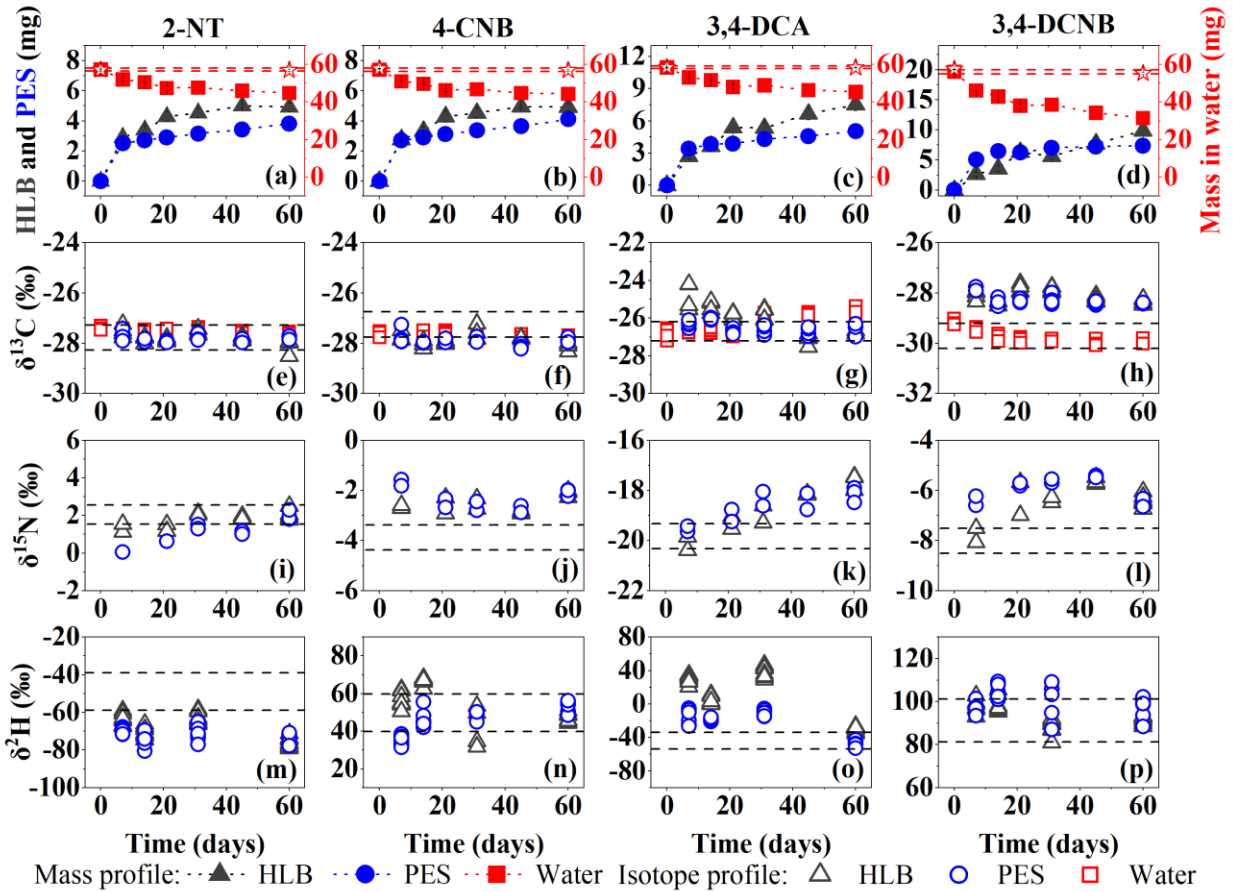
262 *Carbon, nitrogen, and hydrogen isotope profiles*

263 For 2-NT, the $\delta^{13}\text{C}$ values from all three phases, and the $\delta^{15}\text{N}$ value from the HLB phase
264 remained constant and within $\pm 0.5\text{‰}$ of the characterized isotopic signature throughout the
265 exposure time (Figure 1e, 1i). Although the $\delta^{15}\text{N}$ from the PES phase showed an average shift of
266 0.8‰ (i.e., $\delta^{15}\text{N}_{\text{EA/IRMS}} - \delta^{15}\text{N}_{\text{sample}} = 0.8\text{‰}$) for the entire deployment time (Table 1), it became
267 stable with an average shift of 0.4‰ between 31 and 60 days. The $\delta^2\text{H}$ values were depleted in
268 ^2H throughout the deployment time (Figure 1m) compared to the EA/IRMS characterized value,
269 with a constant shift of 19 and 24‰ for the HLB and PES phases, respectively. However, overall
270 the average shifts from both PES and HLB phases were similar, i.e., within a band of 5‰ (Table
271 1).

272 For 4-CNB, the $\delta^{13}\text{C}$ values from both the HLB and PES phases were relatively depleted in ^{13}C
273 compared to the characterized value (Figure 1f). A similar average shift of 0.6 and 0.7‰ was
274 observed in the HLB and PES phases (Table 1), respectively, over the course of the experiment.
275 Changes in $\delta^{13}\text{C}$ from the water phase were insignificant. The obtained $\delta^{15}\text{N}$ values were
276 relatively enriched in ^{15}N (Figure 1i) with an average shift of -1.3 and -1.6‰ for the HLB and
277 PES phases, respectively (Table 1). However, the magnitude of the shift for both C and N was
278 constant and independent of the deployment time. The obtained $\delta^2\text{H}$ values from both the HLB
279 and PES phases showed some instability up to 14 days (Figure 1n) but the overall shift remained
280 within $\pm 5\text{‰}$ for both phases (Table 1).

281 For 3,4-DCA, the average shift in $\delta^{13}\text{C}$ values from the water and PES phases was $<\pm 0.5\text{‰}$
282 (Table 1), although a slight enrichment in ^{13}C in water was noticeable after 31 days (Figure 1g).
283 The $\delta^{13}\text{C}$ values from the HLB phase were enriched in ^{13}C during the initial uptake phase (day 0
284 to 31) and eventually reached isotopic equilibrium after day 31 (Figure 1g). If only the $\delta^{13}\text{C}$
285 values from day 31 onward were considered, the average HLB phase $\delta^{13}\text{C}$ value became $-26.6 \pm$
286 0.5‰ with a $<0.5\text{‰}$ shift from the characterized pure standard. The $\delta^{15}\text{N}$ values from the HLB
287 and PES phases were enriched with ^{15}N over the course of the deployment time (Figure 1k), and
288 reached a constant shift of -1.7 and -1.5‰ , respectively if averaged between 31 to 60 days. A
289 similar trend was observed for $\delta^2\text{H}$ where both phases were enriched with heavier ^2H and an
290 apparent isotopic equilibrium was only obtained at day 60 (Figure 1o). However, it should be
291 noted that the day 0 isotope signature of the water phase had a significant shift of -23.8‰ from
292 the EA/IRMS value (Table 1).

293 For 3,4-DCNB, the $\delta^{13}\text{C}$ values were enriched with ^{13}C (Figure 1h) and showed a constant and
294 reproducible average shift of -1.6 and -1.4‰ for the HLB and PES phases, respectively,
295 throughout the exposure time (Table 1). However, $\delta^{13}\text{C}$ values from the water phase remained
296 within analytical uncertainty, i.e., $\pm 0.5\text{‰}$ (Figure 1h). A similar trend was observed for $\delta^{15}\text{N}$ and
297 the average shift from the both phases were also comparable (Figure 1l, Table 1). The $\delta^2\text{H}$ values
298 were stable for 60 days with negligible average shift from the characterized value ($<\pm 5\text{‰}$)
299 (Figure 1p, Table 1).



300

301 Figure 1 Analyte mass (a-d) in HLB (▲), PES (●), and water (■) phases, and the corresponding
 302 $\delta^{13}\text{C}$ (e-h), $\delta^{15}\text{N}$ (i-l), and $\delta^2\text{H}$ (m-p) values in HLB (Δ), PES (\circ), and water (\square) phases over time
 303 for: 2-NT, 4-CNB, 3,4-DCA, and 3,-4-DCNB. In (a) to (d), the horizontal red dashed lines
 304 represent ± 1 standard deviation of the measured initial spiked mass from all sacrificial setups,
 305 and the open red stars represent the average mass measured from positive controls at days 0 and
 306 60. The error bars are ± 1 standard deviation from duplicate experiments, and the dotted lines are
 307 added to guide the observed trend (a-d). Isotope values of duplicate injections from duplicate
 308 setup are reported without averaging (note that these 4 data points sometimes overlapped for
 309 $\delta^{13}\text{C}$ and $\delta^2\text{H}$; whereas $\delta^{15}\text{N}$ are reported for one replicate). The horizontal black dashed lines

310 represent the total analytical uncertainty of $\pm 0.5\%$ for $\delta^{13}\text{C}$ and $\delta^{15}\text{N}$, and $\pm 10\%$ for $\delta^2\text{H}$ around
 311 the characterized values by EA/IRMS.

312 Table 1 Average δ (‰) values calculated from all sampling points for different phases and the
 313 corresponding average shift ($\Delta\delta$) from the EA/IRMS-characterized values

Analyte	EA	HLB		PES		Water	
		$\delta^{13}\text{C}^*$	$\Delta\delta^{13}\text{C}^{**}$	$\delta^{13}\text{C}^*$	$\Delta\delta^{13}\text{C}^{**}$	$\delta^{13}\text{C}^*$	$\Delta\delta^{13}\text{C}^{**}$
2-NT	-27.8 ± 0.1	-27.8 ± 0.2	0	-27.8 ± 0.1	0	-27.5 ± 0.1	-0.3
4-CNB	-27.3 ± 0.1	-27.9 ± 0.2	0.6	-27.9 ± 0.2	0.7	-27.6 ± 0.1	0.4
3,4-DCA	-26.7 ± 0.2	-26.0 ± 0.8	-0.7	-26.5 ± 0.3	-0.2	-26.3 ± 0.5	-0.4
3,4-DCNB	-29.7 ± 0.03	-28.1 ± 0.3	-1.6	-28.3 ± 0.2	-1.4	-29.7 ± 0.3	0
		$\delta^{15}\text{N}^*$	$\Delta\delta^{15}\text{N}^{**}$	$\delta^{15}\text{N}^*$	$\Delta\delta^{15}\text{N}^{**}$	$\delta^{15}\text{N}$	$\Delta\delta^{15}\text{N}$
2-NT	2.1 ± 0.03	1.8 ± 0.4	0.2	1.4 ± 0.7	0.7	nd	nd
4-CNB	-3.9 ± 0.02	-2.6 ± 0.3	-1.3	-2.3 ± 0.4	-1.6	nd	nd
3,4-DCA	-19.8 ± 0.1	-18.7 ± 1.0	-1.1	-18.6 ± 0.6	-1.2	nd	nd
3,4-DCNB	-8.0 ± 0.03	-6.7 ± 0.7	-1.6	-6.0 ± 0.5	-2.0	nd	nd
		$\delta^2\text{H}^*$	$\Delta\delta^2\text{H}^{**}$	$\delta^2\text{H}^*$	$\Delta\delta^2\text{H}^{**}$	$\delta^2\text{H}^{***}$	$\Delta\delta^2\text{H}^{**}$
2-NT	-48.9 ± 0.3	-67.8 ± 4.6	18.9	-73.2 ± 4.0	24.1	-53.2 ± 1.9	4.3
4-CNB	49.8 ± 0.6	54.4 ± 8.2	-4.6	45.9 ± 6.0	3.9	47.3 ± 1.7	2.5
3,4-DCA	-43.7 ± 1.5	11.0 ± 28.2	-54.7	-23.4 ± 12.7	-20.3	-19.9 ± 1.8	-23.8
3,4-DCNB	91.2 ± 0.5	93.0 ± 4.8	-1.8	100.5 ± 3.6	-9.3	92.1 ± 3.4	-0.9

* Average of all measurement ± 1 standard deviation

** $\Delta\delta = \delta^{\text{h}}\text{X}_{\text{EA/IRMS}} - \text{Average } \delta^{\text{h}}\text{X}$ obtained by GC/IRMS for the corresponding phase (where “h” is for heavy isotope, and X is for an element, i.e., C, N, or H)

*** Day 0 isotope signature in water

nd: not determined

314

315 3.3 Field evaluation of POCIS and grab sampling

316 We compared *in situ* isotope signatures obtained by SPE and POCIS from a pilot constructed
 317 wetland to evaluate the performance of the POCIS-CSIA method under environmental
 318 conditions. Only DCA isomers were present at that site; therefore, the comparison is based on
 319 2,3- and 3,4-DCA. The $\delta^{13}\text{C}$ obtained by SPE was $-31.4 \pm 0.1\%$, and $-27.3 \pm 0.2\%$ for 2,3- and
 320 3,4-DCA, respectively (Table S3, Section S10). The $\delta^{13}\text{C}$ values of 2,3- and 3,4-DCA from
 321 POCIS sorbent and membrane phases showed no significant difference ($< 0.5\%$) from that of the
 322 SPE, expect for a small offset of 0.6% from the membrane phase of 3,4-DCA (Table S3, Section

323 S10). The obtained $\delta^{15}\text{N}$ value of 2,3-DCA was 3.9 ± 0.2 , 2.9 ± 0.5 , and $2.5\pm 0.2\text{‰}$ from SPE, and
324 POCIS sorbent and membrane phases, respectively (Table S4, Section S10). Unlike lab
325 Experiment 2 where the N isotope signature of 3,4-DCA (a comparable isomer to 2,3-DCA) was
326 slightly enriched with heavier ^{15}N in both phases ($\sim 1\text{‰}$) compared to the EA/IRMS signature,
327 the $\delta^{15}\text{N}$ values of 2,3-DCA from the field POCIS were slightly enriched with lighter ^{14}N
328 compared to SPE. However, the observed differences in $\delta^{15}\text{N}$ values between grab sampling and
329 POCIS were $\sim 1\text{‰}$, which is two times the analytical uncertainty for N and thus likely to be
330 considered indistinguishable from the SPE-obtained isotope signatures in the field. Finally, no
331 significant differences were observed in the $\delta^{13}\text{C}$ values of the stainless-steel and copper casings
332 (within $\pm 0.5\text{‰}$); no data were available for H or N isotopes.

333

334 **3.4 Quality assurance and quality control (QA/QC)**

335 No background contamination was observed from the controls and blanks. Total mass loss of
336 each analyte from the water phase was $< 5\%$ during laboratory experiments (positive controls).
337 The standard deviations from replicate injections of the same sample and the duplicate
338 experimental setups were within the analytical uncertainty of each isotope. The only exception
339 was for the HLB phase of 3,4-DCA at day 7 for C and 3,4-DCNB at day 21 for N (Figure 1g, 1l).
340 Compared to the overall data, it is likely an artefact related to the initial rapid adsorption on
341 POCIS. The method-induced isotope fractionation for the PES phase extraction (Table S5,
342 Section S11) and for the SPE method used for the laboratory and field water extractions were
343 negligible (Suchana et al. SPE paper).

344

345 **4. Discussion**

346 **4.1 Compatibility of POCIS with C-, N-, and H-CSIA**

347 Carbon isotope equilibrium of 2-NT was observed within 7 days (Figure 1e), although
348 concentration equilibrium needed approximately 31 days (Figure 1a). Initially, a temporal trend
349 in $\delta^{13}\text{C}$ values was observed for 3,4-DCA; nevertheless, the obtained isotope values were within
350 the characterized signature as POCIS uptake approached near-equilibrium after 31 days (Figure
351 1c, 1g). Thus, POCIS is compatible with C-CSIA without further considerations for 2-NT and
352 3,4-DCA. For 4-CNB and 3,4-DCNB, while a significant shift in carbon isotope signature was
353 evident, it was constant and reproducible throughout the deployment (Figure 1f, 1h). A similar
354 constant and reproducible shift in $\delta^{13}\text{C}$ was observed for hexane (1.4‰), benzene (1.2‰), and
355 trichloroethylene (0.9‰) in the Waterloo Membrane Sampler.¹⁷ This sampler was successfully
356 applied at contaminated sites for CSIA by correcting the reproducible shift of $\delta^{13}\text{C}$ associated
357 with the gas-phase passive sampling technique.^{17,18} However, as the carbon isotope fractionation
358 in POCIS was <1‰ for 4-CNB, i.e., 2 times the total analytical uncertainty of $\delta^{13}\text{C}$, and <2‰ for
359 3,4-DCNB, i.e., the recommended maximal isotope shift for field interpretation,¹⁰ we do not
360 recommend isotopic correction for carbon during field application of the POCIS-CSIA
361 technique.

362 A significant shift was observed for nitrogen isotope for all compounds for both sorbent and
363 membrane phases (0.8 to 2‰), except the sorbent phase of 2-NT (<0.5‰). However, the shifts
364 were constant after 21 days. The total shift was $\leq 2\text{‰}$ and thus no isotopic correction is
365 recommended for N isotope during field application.

366 The average hydrogen isotope signature of 4-CNB and 3,4-DCNB from POCIS differed be less
367 than 10‰ from the EA/IRMS signature, i.e., 2 times the total analytical uncertainty for $\delta^2\text{H}$

368 ($\pm 5\%$) (Table 1). Thus, no correction is recommended for 4-CNB and 3,4-DCNB. However, a
369 significant shift of $>10\%$ for 2-NT and 3,4-DCA was observed (Table 1). However, the shift for
370 2-NT was constant throughout the deployment time for both phases (standard deviation $<5\%$)
371 for which a correction factor, similarly as the Waterloo Membrane Sampler,¹⁷ could be applied
372 for field application. The $\delta^2\text{H}$ for 3,4-DCA was mostly too variable between the sampling times
373 which might require further mechanistic study to interpret this behaviour.

374

375 **4.2 Diffusion- and adsorption-induced isotope fractionation**

376 Analyte mass transfer from the water column to POCIS receiving phases involves multistep
377 diffusion, i.e., in the water boundary layer, pore waters in PES and HLB, and in polymer matrix
378 involving intra-particle and interstitial diffusion.^{27,28} Thus, three phenomena could lead to
379 isotope fractionation during POCIS preconcentration: (i) aqueous-phase diffusion; (ii) diffusion
380 in PES and HLB; and (iii) adsorption on PES and HLB.

381 Diffusion and subsequent adsorption of molecules incorporating heavy isotopes are expected to
382 be slower than for those made of light isotopes, resulting in an enrichment with lighter isotopes
383 in the POCIS receiving phases as the overall direction of mass transfer is towards the POCIS.

384 Diffusion typically does not cause significant isotope fractionation^{13,19,29} considering typical
385 temporal and spatial sampling regimes in the field. However, the static experimental system used
386 in this study could likely cause a solute gradient in the water boundary layer that might be
387 responsible for diffusion-induced isotope fractionation. Since all target compounds have
388 comparable molecular mass, water diffusivity, $\log K_{ow}$, membrane-water partition coefficient
389 ($\log K_{PES-water}$), and Freundlich membrane adsorption coefficients ($\log K_F$, n_f) values (Table S1),

390 similar isotope fractionation due to diffusion in all phases should have been observed for all
391 compounds. Most importantly, when a significant shift was observed, POCIS receiving phases
392 were predominantly enriched with the heavier isotopes, which is unlikely the results of a
393 diffusion-induced process. Therefore, the observed isotope fractionation in POCIS might be
394 explained by the adsorption steps in the PES and HLB phases.

395 To directly evaluate potential isotope fractionation specifically associated with the PES phase,
396 we compared the results from standard POCIS configuration (Experiment 2, Figure 1) to that of
397 the HLB-free POCIS configuration (Experiment 3, Table S2, Section S9). The $\delta^{13}\text{C}$ values of
398 3,4-DCNB from the PES phase showed no significant shift ($<0.5\text{‰}$) in the HLB-free POCIS
399 (Table S2), thus indicating that the observed carbon isotope shift from Experiment 2 was likely
400 associated with the HLB phase adsorption. Electrostatic interactions between aromatic
401 compounds and PES involve H-bond formation and π - π interactions,³⁰⁻³³ where additional
402 aromatic stacking could occur for compounds having electron-withdrawing substituents, e.g., Cl-,
403 NO_2 .^{34,35} However, such interactions between (di)chlorobenzenes and polysulfone membrane
404 previously showed negligible carbon isotope fractionation under equilibrium sorption
405 condition.¹⁹ As PES membrane contains similar repeating units as polysulfone membranes,
406 adsorption on PES did not cause carbon isotope fractionation.

407 Adsorption on HLB is mainly favored by dipole-dipole and hydrogen bond interactions, but
408 electron lone pair interactions with HLB could also be present for polar compounds^{36,37}. The lone
409 pair of electrons from Cl- and NO_2 - substituents of 3,4-DCNB possibly caused stronger
410 intermolecular interactions with the HLB phase resulting in significant carbon isotope
411 fractionation. Multistep sorption and successive partitioning steps were previously reported to
412 cause preferential accumulation of lighter carbon isotope on the sorbent phase depending on the

413 specific intermolecular interactions.³⁸⁻⁴⁰ However, the observed shifts in POCIS for most
414 compounds were counter-intuitive as the isotope signature in HLB and PES phases were mostly
415 enriched with heavier ¹³C (Figure 1h), ¹⁵N (Figure 1j, 1k, 1l), and ²H (1o).

416 Inverse isotope effects during adsorption processes were reported precisely when a molecule
417 binds to a non-biological binding pocket and has been termed as binding isotope effects (BIEs).⁴¹
418 For example, inverse BIEs were observed for *p*-xylene and carbon tetrachloride while binding in
419 a dimeric capsule molecule.⁴² Gibb and coworkers studied the C-H···X-R hydrogen bond
420 interaction between a cavitated sorbent and a variety of halogenated compounds. Depending on
421 the halogen atom and the size of the sorbent, either normal or inverse BIEs were observed.^{41,43} It
422 is plausible that the strong C-H···X-R interaction between the benzyl moiety of HLB and the Cl
423 atoms of the compounds could lead to the observed inverse isotope fractionation during the
424 adsorption/binding processes. The role of Cl atom for the inverse isotope effect is somewhat
425 evident from our work as we observed the least inverse effect for 2-NT which does not contain
426 Cl atom.

427 Similar significant inverse carbon and nitrogen isotope fractionation were observed during direct
428 immersion solid-phase microextraction (SPME) of several NO₂- and NH₂- substituted
429 chlorobenzenes.⁴⁴ Although it was suggested as an artefact of reactor oxidation state,⁴⁴ it could
430 also be a BIEs due to the C-H···X-R interaction between the polyacrylate SPME fiber and
431 halogenated compounds. Analyte accumulation in direct immersion SPME and POCIS is similar,
432 where aqueous phase compounds diffuse and adsorb on the sorbent phase. However, interactions
433 and associated isotope fractionation are highly dependent on the specific analyte-sorbent pair
434 and, thus, difficult to postulate.

435

436 4.3 Potential of CSIA at trace levels using POCIS

437 We estimated the minimum water concentration ($C_{w, \min}$) required for precise and accurate C-, H-
438 and N-CSIA, which ranged from 5 to 2 $\mu\text{g/L}$ for C, 518 to 307 $\mu\text{g/L}$ for H, and 1901 to 418 $\mu\text{g/L}$
439 for N after a 60-day deployment if the accumulated mass in the HLB phase (conventional POCIS
440 sink) of one POCIS were considered (Table S6, Section S12). The obtained C-CSIA method
441 quantification limits of the target compounds using POCIS were comparable to the 10 L of water
442 extraction using SPE.¹⁵ We also calculated the projected $C_{w, \min}$ of C-CSIA for other polar
443 organic compounds ($1.4 \leq \log K_{ow} \leq 4.5$), such as pesticides, fungicides, pharmaceuticals, and
444 anticorrosives, which ranged between 0.1 to 1.5 $\mu\text{g/L}$ for the HLB phase of one POCIS (Table
445 S7, Section S12).

446 Both HLB and PES phases acted as significant sinks for the target compounds (Figure 1a-1d).
447 Besides, differences in average δ values obtained from both POCIS phases were $<0.5\text{‰}$ for C
448 and N and $<10\text{‰}$ for H isotopes, even when a significant shift was observed (except for the 3,4-
449 DCA for H) (Table 1). Thus, the recovered mass from both phases could be combined to further
450 lower the CSIA detection limits without introducing isotopic bias. For example, $C_{w, \min}$ for C-
451 CSIA ranged between 1 to 3 $\mu\text{g/L}$ for combined PES and HLB extracts of one POCIS after a 60-
452 day deployment (Table S8, Section S12), which is approximately 50% lower compared to that of
453 the HLB phase alone. POCIS preconcentration also lowered the detection limits for N- and H-
454 CSIA of the target compounds at concentrations down to approximately 200 $\mu\text{g/L}$ and 200-1000
455 $\mu\text{g/L}$, respectively when sorbent and membrane extracts from one POCIS were combined (Table
456 S3). This concept was demonstrated for the field POCIS that allowed us to obtain $\delta^{13}\text{C}$ values at
457 concentration down to $<3 \mu\text{g/L}$ for 2-CNB (Table S3, Section S10) and for $\delta^{15}\text{N}$ at 144 $\mu\text{g/L}$ for

458 3,4-DCA (Table S4, Section S10) using the combined sorbent and membrane extracts of one
459 POCIS; whereas, we could not measure the isotope signatures from the 4-L SPE.

460 Moreover, similar to concentration analysis,²³ combining the PES and HLB extracts from
461 multiple POCIS could potentially lower the CSIA detection limits compared to a single POCIS
462 (Table S8, Section S12). However, we attempted to combine both the sorbent and membrane
463 extracts of three POCIS but the obtained isotope traces were compromised due to the increased
464 background from highly preconcentrated matrix interferences.

465 Based on the observed accumulation of the target compounds by POCIS, three suggestions could
466 be offered to explore POCIS preconcentration for CSIA at the ng/L range. First, more HLB
467 sorbent mass can be added to the POCIS to increase overall adsorption capacity. Studies
468 suggested that sampling rates could be doubled using 600 mg HLB instead of 200 mg in the
469 standard POCIS configuration.⁴⁵ Second, a modified POCIS design can be used to increase the
470 exposure surface area. A rectangular POCIS configuration mainly used for groundwater⁴⁶ has a
471 sampling capacity equivalent to three standard circular POCIS and would be ideal for achieving
472 ng/L range CSIA. Third, selective sorbent can be used in POCIS to increase analyte
473 preconcentration. Various commercially available sorbents, such as OASIS MCX, OASIS MAX,
474 Starta, Chromabond HR-X,⁴⁷⁻⁴⁹ and molecularly imprinted sorbents^{50,51} have been used for
475 increased and selective analyte accumulation in POCIS. Selective sorbents can potentially
476 achieve high *in situ* preconcentration as well as lower background interferences for CSIA.

477

478 **4.4 POCIS conserves isotope signatures in the field**

479 The long deployment time of POCIS in the field, typically between 1 to 4 weeks, can lead to
480 biofilm growth and sediment deposition on the membrane surface. The deposition of suspended
481 materials might cause diffusion-induced isotope fractionation, whereas the biofilm layer might
482 affect the isotope signature due to increased diffusion barrier and potential microbial degradation
483 of the sampled compounds. Our results from scanning electron microscopy and DNA analysis
484 confirmed negligible biofilm formation and the presence of diverse microbial community
485 (maximum abundance <15% for a single genus) on the exposed membrane surface (Figure S3,
486 Section S13). In addition, we did not observe the dominance of microbes known to degrade the
487 target compounds (Figure S3, Section S13). Thus, it is unlikely that biofilm developing on the
488 membranes would contribute to isotope fractionation via either diffusion of chemicals through
489 the biofilm or biotransformation.

490 In addition, similar microbial morphologies and community were present on the membranes
491 from both copper and stainless-steel casings, suggesting that the copper did not prevent microbial
492 attachment (Figure S4, Section 13), although copper mesh is often used for passive samplers to
493 limit biofilm formation.^{52,53} However, significant biofilm formation might be an issue for longer
494 deployment time in other environmental settings. In such cases, composite extracts from multiple
495 POCIS exposed in the water for a short time could be useful.

496

497 **5. Environmental implications**

498 Overall, our results demonstrated that POCIS are compatible with C-, N- and H-CSIA for most
499 target compounds and can potentially be used for CSIA of other emerging polar compounds at
500 trace levels. POCIS has been extensively used for hundreds of polar organic compounds at low

501 environmental concentrations⁵⁴⁻⁵⁶ in wastewater, surface water, groundwater, marine water,
502 wastewater treatment plants, constructed wetlands, and long-term remediation sites.^{23,57} Thus,
503 combining POCIS with CSIA has the potential to enable CSIA application to thousands of polar
504 emerging contaminants present in the environment, such as pesticides, pharmaceuticals, and
505 flame-retardants, possibly at low $\mu\text{g/L}$ to ng/L levels. Therefore, POCIS could be a convenient
506 sample preconcentration technique for C-, H-, and N-CSIA to understand *in situ* transformation
507 of polar emerging contaminants in natural and engineering systems at extremely low
508 concentrations.

509 The results presented here also demonstrate the importance to verify the appropriate sampling
510 time to use POCIS for CSIA. POCIS field deployment time usually varies from one week to four
511 weeks,²³ which aligns well with the sampling time requirement of most target compounds for
512 CSIA. In addition, the measured isotope signature from POCIS will provide a pooled or time-
513 integrated *in situ* information, although we did not observe any significant differences in isotope
514 signatures obtained from POCIS and grab sampling after a 60-day deployment.

515 Lastly, achieving isotopic equilibrium in POCIS could depend on specific analyte-membrane-
516 sorbent interactions and can potentially lead to significant but reproducible isotope fractionation.
517 Thus, careful laboratory and *in situ* evaluation are recommended before applying POCIS-CSIA
518 technique for new compounds. Predictive models could be developed to better understand the
519 intermolecular interactions of PES and HLB with different compound groups. Such models
520 could help evaluate the potential implications of the POCIS-CSIA technique for new compounds
521 that might have special intermolecular interactions with HLB and PES phases.

522

523 **Acknowledgements**

524 We thank Hans-Hermann Richnow and Steffen Kümmel from the Helmholtz Centre for
525 Environmental Research – UFZ, Leipzig, Germany for their help with EA/IRMS measurements.
526 We thank Langping Wu (University of Toronto) for input on the results and GC/IRMS analytical
527 support.

528

529 **References**

- 530 (1) Booth, G. Nitro Compounds, Aromatic. *Ullmann's Encyclopedia of Industrial Chemistry*;
531 Wiley-VCH Verlag GmbH & Co. KGaA: Weinheim, Germany, 2000; pp 301–349.
- 532 (2) Ju, K. S.; Parales, R. E. Application of Nitroarene Dioxygenases in the Design of Novel
533 Strains That Degrade Chloronitrobenzenes. *Microb. Biotechnol.* **2009**, 2 (2 SPEC. ISS.),
534 241–252.
- 535 (3) Elsner, M.; Schwarzenbach, R. P.; Haderlein, S. B. Reactivity of Fe(II)-Bearing Minerals
536 toward Reductive Transformation of Organic Contaminants. *Environ. Sci. Technol.* **2004**,
537 38 (3), 799–807.
- 538 (4) Hussain, S.; Arshad, M.; Springael, D.; Sørensen, S. R.; Bending, G. D.; Devers-
539 Lamrani, M.; Maqbool, Z.; Martin-Laurent, F. Abiotic and Biotic Processes Governing the
540 Fate of Phenylurea Herbicides in Soils: A Review. *Crit. Rev. Environ. Sci. Technol.* **2015**,
541 45 (18), 1947–1998.
- 542 (5) Kaufman, D. D.; Plimmer, J. R.; Klingebiel, U. I. Microbial Oxidation of 4-Chloroaniline.
543 *J. Agric. Food Chem.* **1973**, 21 (1), 127–132.

- 544 (6) United States Environmental Protection Agency (US EPA). Priority pollutant list
545 [https://www.epa.gov/sites/production/files/2015-09/documents/priority-pollutant-list-](https://www.epa.gov/sites/production/files/2015-09/documents/priority-pollutant-list-epa.pdf)
546 [epa.pdf](https://www.epa.gov/sites/production/files/2015-09/documents/priority-pollutant-list-epa.pdf) (accessed Jan 29, 2022).
- 547 (7) Spain, J. C.; Hughes, J. B.; Knackmuss, H.-J.; Hughes, J. B.; Knackmuss, H.-J.
548 *Biodegradation of Nitroaromatic Compounds and Explosives*; Hughes, J., Spain, J.,
549 Knackmuss, H.-J., Eds.; CRC Press, 2000.
- 550 (8) Lekkas, T.; Kolokythas, G.; Nikolaou, A.; Kostopoulou, M.; Kotrikla, A.; Gatidou, G.;
551 Thomaidis, N. S.; Golfinopoulos, S.; Makri, C.; Babos, D.; Vagi, M.; Stasinakis, A.;
552 Petsas, A.; Lekkas, D. F. Evaluation of the Pollution of the Surface Waters of Greece from
553 the Priority Compounds of List II, 76/464/EEC Directive, and Other Toxic Compounds.
554 *Environ. Int.* **2004**, *30* (8), 995–1007.
- 555 (9) Schwarzbauer, J.; Ricking, M. Non-Target Screening Analysis of River Water as
556 Compound-Related Base for Monitoring Measures. *Environ. Sci. Pollut. Res.* **2010**, *17* (4),
557 934–947.
- 558 (10) Hunkeler, D.; Meckenstock, R. U.; Sherwood Lollar, B.; Schmidt, T. C.; Wilson, J. T. A
559 Guide for Assessing Biodegradation and Source Identification of Organic Ground Water
560 Contaminants Using Compound Specific Isotope Analysis (CSIA). *USEPA Publ.* **2008**,
561 *EPA 600/R-* (December), 1–82.
- 562 (11) Harrington, R. R.; Poulson, S. R.; Drever, J. I.; Colberg, P. J. S.; Kelly, E. F. Carbon
563 Isotope Systematics of Monoaromatic Hydrocarbons: Vaporization and Adsorption
564 Experiments. *Org. Geochem.* **1999**, *30* (8 A), 765–775.
- 565 (12) Slater, G. F.; Ahad, J. M. E.; Sherwood Lollar, B.; Allen-King, R.; Sleep, B. Carbon

- 566 Isotope Effects Resulting from Equilibrium Sorption of Dissolved VOCs. *Anal. Chem.*
567 **2000**, *72* (22), 5669–5672.
- 568 (13) Xu, B. S.; Sherwood Lollar, B.; Passeport, E.; Sleep, B. E. Diffusion Related Isotopic
569 Fractionation Effects with One-Dimensional Advective-Dispersive Transport. *Sci. Total*
570 *Environ.* **2016**, *550*, 200–208.
- 571 (14) Melsbach, A.; Pittois, D.; Bayerle, M.; Daubmeier, M.; Meyer, A. H.; Hölzer, K.; Gallé,
572 T.; Elsner, M. Isotope Fractionation of Micropollutants during Large-Volume Extraction:
573 Heads-up from a Critical Method Evaluation for Atrazine, Desethylatrazine and 2,6-
574 Dichlorobenzamide at Low Ng/L Concentrations in Groundwater. *Isotopes Environ.*
575 *Health Stud.* **2021**, *57* (1), 35–52.
- 576 (15) Torrentó, C.; Bakkour, R.; Glauser, G.; Melsbach, A.; Ponsin, V.; Hofstetter, T. B.;
577 Elsner, M.; Hunkeler, D. Solid-Phase Extraction Method for Stable Isotope Analysis of
578 Pesticides from Large Volume Environmental Water Samples. *Analyst* **2019**, *144* (9),
579 2898–2908.
- 580 (16) Wang, Y.; Huang, Y.; Huckins, J. N.; Petty, J. D. Compound-Specific Carbon and
581 Hydrogen Isotope Analysis of Sub-Parts per Billion Level Waterborne Petroleum
582 Hydrocarbons. *Environ. Sci. Technol.* **2004**, *38* (13), 3689–3697.
- 583 (17) Goli, O.; Górecki, T.; Mugammar, H. T.; Marchesi, M.; Aravena, R. Evaluation of the
584 Suitability of the Waterloo Membrane Sampler for Sample Preconcentration before
585 Compound-Specific Isotope Analysis. *Environ. Technol. Innov.* **2017**, *7*, 141–151.
- 586 (18) BenIsrael, M.; Wanner, P.; Aravena, R.; Parker, B. L.; Haack, E. A.; Tsao, D. T.;
587 Dunfield, K. E. Toluene Biodegradation in the Vadose Zone of a Poplar Phytoremediation

- 588 System Identified Using Metagenomics and Toluene-Specific Stable Carbon Isotope
589 Analysis. *Int. J. Phytoremediation* **2019**, *21* (1), 60–69.
- 590 (19) Passeport, E.; Landis, R.; Mundle, S. O. C.; Chu, K.; Mack, E. E.; Lutz, E.; Sherwood
591 Lollar, B. Diffusion Sampler for Compound Specific Carbon Isotope Analysis of
592 Dissolved Hydrocarbon Contaminants. *Environ. Sci. Technol.* **2014**, *48* (16), 9582–9590.
- 593 (20) Passeport, E.; Landis, R.; Lacrampe-Couloume, G.; Lutz, E. J.; Erin Mack, E.; West, K.;
594 Morgan, S.; Sherwood Lollar, B. Sediment Monitored Natural Recovery Evidenced by
595 Compound Specific Isotope Analysis and High-Resolution Pore Water Sampling.
596 *Environ. Sci. Technol.* **2016**, *50* (22), 12197–12204.
- 597 (21) Gilevska, T.; Passeport, E.; Shayan, M.; Seger, E.; Lutz, E. J.; West, K. A.; Morgan, S. A.;
598 Mack, E. E.; Sherwood Lollar, B. Determination of in Situ Biodegradation Rates via a
599 Novel High Resolution Isotopic Approach in Contaminated Sediments. *Water Res.* **2019**,
600 *149*, 632–639.
- 601 (22) Alvarez, D. A.; Petty, J. D.; Huckins, J. N.; Jones-Lepp, T. L.; Getting, D. T.; Goddard, J.
602 P.; Manahan, S. E. Development of a Passive, in Situ, Integrative Sampler for Hydrophilic
603 Organic Contaminants in Aquatic Environments. *Environ. Toxicol. Chem.* **2004**, *23* (7),
604 1640–1648.
- 605 (23) Alvarez, D. A. Guidelines for the Use of the Semi Permeable Membrane Device (SPMD)
606 and the Polar Organic Chemical Integrative Sampler (POCIS) in Environmental
607 Monitoring. *Tech. Methods* **2010**, 1–D4, 28 p.
- 608 (24) Grass, G.; Rensing, C.; Solioz, M. Metallic Copper as an Antimicrobial Surface. *Appl.*
609 *Environ. Microbiol.* **2011**, *77* (5), 1541–1547.

- 610 (25) Sherwood Lollar, B.; Hirschorn, S. K.; Chartrand, M. M. G.; Lacrampe-Couloume, G. An
611 Approach for Assessing Total Instrumental Uncertainty in Compound-Specific Carbon
612 Isotope Analysis: Implications for Environmental Remediation Studies. *Anal. Chem.*
613 **2007**, 79 (9), 3469–3475.
- 614 (26) Brand, W. A.; Coplen, T. B. Stable Isotope Deltas: Tiny, yet Robust Signatures in Nature.
615 *Isotopes Environ. Health Stud.* **2012**, 48 (3), 393–409.
- 616 (27) Vermeirssen, E. L. M.; Dietschweiler, C.; Escher, B. I.; Van Der Voet, J.; Hollender, J.
617 Transfer Kinetics of Polar Organic Compounds over Polyethersulfone Membranes in the
618 Passive Samplers POCIS and Chemcatcher. *Environ. Sci. Technol.* **2012**, 46 (12), 6759–
619 6766.
- 620 (28) Belles, A.; Pardon, P.; Budzinski, H. Development of an Adapted Version of Polar
621 Organic Chemical Integrative Samplers (POCIS-Nylon). *Anal. Bioanal. Chem.* **2014**, 406
622 (4), 1099–1110.
- 623 (29) Wanner, P.; Hunkeler, D. Carbon and Chlorine Isotopologue Fractionation of Chlorinated
624 Hydrocarbons during Diffusion in Water and Low Permeability Sediments. *Geochim.*
625 *Cosmochim. Acta* **2015**, 157, 198–212.
- 626 (30) Bope, C. D.; Nalaparaju, A.; Ng, C. K.; Cheng, Y.; Lu, L. Molecular Simulation on the
627 Interaction of Ethinylestradiol (EE2) with Polymer Membranes in Wastewater
628 Purification. *Mol. Simul.* **2018**, 44 (8), 638–647.
- 629 (31) Endo, S.; Matsuura, Y. Characterizing Sorption and Permeation Properties of Membrane
630 Filters Used for Aquatic Integrative Passive Samplers. *Environ. Sci. Technol.* **2018**, 52 (4),
631 2118–2125.

- 632 (32) Ng, C. K.; Bope, C. D.; Nalaparaju, A.; Cheng, Y.; Lu, L.; Wang, R.; Cao, B.
633 Concentrating Synthetic Estrogen 17 α -Ethinylestradiol Using Microporous
634 Polyethersulfone Hollow Fiber Membranes: Experimental Exploration and Molecular
635 Simulation. *Chem. Eng. J.* **2017**, *314*, 80–87.
- 636 (33) Schäfer, A. I.; Akanyeti, I.; Semião, A. J. C. Micropollutant Sorption to Membrane
637 Polymers: A Review of Mechanisms for Estrogens. *Adv. Colloid Interface Sci.* **2011**, *164*
638 (1–2), 100–117.
- 639 (34) Cockroft, S. L.; Hunter, C. A.; Lawson, K. R.; Perkins, J.; Urch, C. J. Electrostatic Control
640 of Aromatic Stacking Interactions. *J. Am. Chem. Soc.* **2005**, *127* (24), 8594–8595.
- 641 (35) Cockroft, S. L.; Perkins, J.; Zonta, C.; Adams, H.; Spey, S. E.; Low, C. M. R.; Vinter, J.
642 G.; Lawson, K. R.; Urch, C. J.; Hunter, C. A. Substituent Effects on Aromatic Stacking
643 Interactions. *Org. Biomol. Chem.* **2007**, *5* (7), 1062–1080.
- 644 (36) Dias, N. C.; Poole, C. F. Mechanistic Study of the Sorption Properties of Oasis® HLB and
645 Its Use in Solid-Phase Extraction. *Chromatographia* **2002**, *56* (5–6), 269–275.
- 646 (37) Bäuerlein, P. S.; Mansell, J. E.; Ter Laak, T. L.; De Voogt, P. Sorption Behavior of
647 Charged and Neutral Polar Organic Compounds on Solid Phase Extraction Materials:
648 Which Functional Group Governs Sorption? *Environ. Sci. Technol.* **2012**, *46* (2), 954–
649 961.
- 650 (38) Kopinke, F. D.; Georgi, A.; Voskamp, M.; Richnow, H. H. Carbon Isotope Fractionation
651 of Organic Contaminants Due to Retardation on Humic Substances: Implications for
652 Natural Attenuation Studies in Aquifers. *Environ. Sci. Technol.* **2005**, *39* (16), 6052–6062.

- 653 (39) Imfeld, G.; Kopinke, F. D.; Fischer, A.; Richnow, H. H. Carbon and Hydrogen Isotope
654 Fractionation of Benzene and Toluene during Hydrophobic Sorption in Multistep Batch
655 Experiments. *Chemosphere* **2014**, *107*, 454–461.
- 656 (40) Wanner, P.; Parker, B. L.; Chapman, S. W.; Aravena, R.; Hunkeler, D. Does Sorption
657 Influence Isotope Ratios of Chlorinated Hydrocarbons under Field Conditions? *Appl.*
658 *Geochemistry* **2017**, *84*, 348–359.
- 659 (41) Świderek, K.; Paneth, P. Binding Isotope Effects. *Chem. Rev.* **2013**, *113* (10), 7851–7879.
- 660 (42) Rechavi, D.; Scarso, A.; Rebek, J. Isotopomer Encapsulation in a Cylindrical Molecular
661 Capsule: A Probe for Understanding Noncovalent Isotope Effects on a Molecular Level. *J.*
662 *Am. Chem. Soc.* **2004**, *126* (25), 7738–7739.
- 663 (43) Laughrey, Z. R.; Upton, T. G.; Gibb, B. C. A Deuterated Deep-Cavity Cavitand Confirms
664 the Importance of C-H···X-R Hydrogen Bonds in Guest Binding. *Chem. Commun.* **2006**,
665 No. 9, 970–972.
- 666 (44) Berg, M.; Bolotin, J.; Hofstetter, T. B. Compound-Specific Nitrogen and Carbon Isotope
667 Analysis of Nitroaromatic Compounds in Aqueous Samples Using Solid-Phase
668 Microextraction Coupled to GC/IRMS. *Anal. Chem.* **2007**, *79* (6), 2386–2393.
- 669 (45) Fauvelle, V.; Mazzella, N.; Belles, A.; Moreira, A.; Allan, I. J.; Budzinski, H.
670 Optimization of the Polar Organic Chemical Integrative Sampler for the Sampling of
671 Acidic and Polar Herbicides. *Anal. Bioanal. Chem.* **2014**, *406* (13), 3191–3199.
- 672 (46) Environmental Sampling Technologies. Environmental Sampling Technologies - The
673 Leader in Polar Organic Chemical Integrative Samplers (POCIS) <https://est->

- 674 lab.com/pocis.php (accessed Feb 2, 2022).
- 675 (47) Li, H.; Helm, P. A.; Paterson, G.; Metcalfe, C. D. The Effects of Dissolved Organic
676 Matter and PH on Sampling Rates for Polar Organic Chemical Integrative Samplers
677 (POCIS). *Chemosphere* **2011**, *83* (3), 271–280.
- 678 (48) Fauvelle, V.; Mazzella, N.; Delmas, F.; Madarassou, K.; Eon, M.; Budzinski, H. Use of
679 Mixed-Mode Ion Exchange Sorbent for the Passive Sampling of Organic Acids by Polar
680 Organic Chemical Integrative Sampler (POCIS). *Environ. Sci. Technol.* **2012**, *46* (24),
681 13344–13353.
- 682 (49) Kaserzon, S. L.; Kennedy, K.; Hawker, D. W.; Thompson, J.; Carter, S.; Roach, A. C.;
683 Booij, K.; Mueller, J. F. Development and Calibration of a Passive Sampler for
684 Perfluorinated Alkyl Carboxylates and Sulfonates in Water. *Environ. Sci. Technol.* **2012**,
685 *46* (9), 4985–4993.
- 686 (50) Berho, C.; Claude, B.; Coisy, E.; Togola, A.; Bayouhd, S.; Morin, P.; Amalric, L.
687 Laboratory Calibration of a POCIS-like Sampler Based on Molecularly Imprinted
688 Polymers for Glyphosate and AMPA Sampling in Water. *Anal. Bioanal. Chem.* **2017**, *409*
689 (8), 2029–2035.
- 690 (51) Berho, C.; Robert, S.; Coureau, C.; Coisy, E.; Berrehouc, A.; Amalric, L.; Bruchet, A.
691 Estimating 42 Pesticide Sampling Rates by POCIS and POCIS-MIP Samplers for
692 Groundwater Monitoring: A Pilot-Scale Calibration. *Environ. Sci. Pollut. Res.* **2020**, *27*
693 (15), 18565–18576.
- 694 (52) Alvarez, D. A.; Maruya, K. A.; Dodder, N. G.; Lao, W.; Furlong, E. T.; Smalling, K. L.
695 Occurrence of Contaminants of Emerging Concern along the California Coast (2009-10)

- 696 Using Passive Sampling Devices. *Mar. Pollut. Bull.* **2014**, *81* (2), 347–354.
- 697 (53) Vrana, B.; Allan, I. J.; Greenwood, R.; Mills, G. A.; Dominiak, E.; Svensson, K.;
698 Knutsson, J.; Morrison, G. Passive Sampling Techniques for Monitoring Pollutants in
699 Water. *TrAC - Trends Anal. Chem.* **2005**, *24* (10), 845–868.
- 700 (54) Harman, C.; Allan, I. J.; Vermeirssen, E. L. M. Calibration and Use of the Polar Organic
701 Chemical Integrative Sampler-a Critical Review. *Environ. Toxicol. Chem.* **2012**, *31* (12),
702 2724–2738.
- 703 (55) Alvarez, D.; Perkins, S.; Nilsen, E.; Morace, J. Spatial and Temporal Trends in
704 Occurrence of Emerging and Legacy Contaminants in the Lower Columbia River 2008-
705 2010. *Sci. Total Environ.* **2014**, *484* (1), 322–330.
- 706 (56) Fent, K.; Zenker, A.; Rapp, M. Widespread Occurrence of Estrogenic UV-Filters in
707 Aquatic Ecosystems in Switzerland. *Environ. Pollut.* **2010**, *158* (5), 1817–1824.
- 708 (57) Vallejo, A.; Prieto, A.; Moeder, M.; Usobiaga, A.; Zuloaga, O.; Etxebarria, N.; Paschke,
709 A. Calibration and Field Test of the Polar Organic Chemical Integrative Samplers for the
710 Determination of 15 Endocrine Disrupting Compounds in Wastewater and River Water
711 with Special Focus on Performance Reference Compounds (PRC). *Water Res.* **2013**, *47*
712 (8), 2851–2862.

713